Discrete Multitone Modulation for Maximizing Transmission Rate in Step-Index Plastic Optical Fibres

Discrete Multitone Modulation for Maximizing Transmission Rate in Step-Index Plastic Optical Fibers

S. C. Jeffrey Lee, *Student Member, IEEE*, Florian Breyer, *Student Member, IEEE*, Sebastian Randel, *Member, IEEE*, Roberto Gaudino, *Member, IEEE*, Gabriella Bosco, *Member, IEEE*, Andreas Bluschke, *Member, IEEE*, Michael Matthews, Philipp Rietzsch, Rainer Steglich, Henrie P. A. van den Boom, and Antonius M. J. Koonen, *Fellow, IEEE*

***Abstract*—The use of standard 1-mm core-diameter step-index plastic optical fiber (SI-POF) has so far been mainly limited to distances of up to 100 m and bit-rates in the order of 100 Mbit/s. By use of digital signal processing, transmission performance of such optical links can be improved. Among the different technical solutions proposed, a promising one is based on the use of discrete multitone (DMT) modulation, directly applied to intensity-modulated, direct detection (IM/DD) SI-POF links. This paper presents an overview of DMT over SI-POF and demonstrates how DMT can be used to improve transmission rate in such IM/DD systems. The achievable capacity of an SI-POF channel is first analyzed theoretically and then validated by experimental results. Additionally, first experimental demonstrations of a real-time DMT over SI-POF system are presented and discussed.**

***Index Terms*—Frequency division multiplexing, multimode waveguides, optical fiber communication, quadrature amplitude modulation (QAM), signal processing, subcarrier multiplexing.**

I. Introduction

DURING the past years, SI-POF has established itself as the preferred alternative transmission medium for robust short-distance data communications in fast-growing markets such as industrial automation networks and multimedia communication in cars. Its main benefits are its robustness to electromagnetic interference and mechanical stress, its ease of installation and connection, its low weight, as well as its low price.

Nowadays, connector-less SI-POF systems are also available on the consumer market for in-house networks, supporting various applications such as, e.g., IP-TV distribution in homes [1]. While today's commercial systems operate at 100 Mbit/s over up to 100 m of SI-POF, next generation systems are expected to carry Gigabit Ethernet data over comparable distances. However, due to its large numerical aperture (NA) of 0.5, the bandwidth of SI-POF is limited to around 50 MHz $\times$ 100 m. This makes the possibility of Gigabit transmission over SI-POF seem unlikely. Nevertheless, several advanced modulation techniques have been proposed recently that make this step feasible [2], [3]. Especially, by combining multicarrier modulation with spectrally efficient quadrature amplitude modulation (QAM), the first demonstration of 1-Gbit/s transmission over 100 m of SI-POF was reported [2].

An efficient digital implementation of multicarrier modulation is orthogonal frequency division multiplexing (OFDM) [4], which is already employed in many wireless communications standards such as Wireless Local Area Networks (WLAN), Worldwide Interoperability for Microwave Access (WiMAX), and terrestrial Digital Video Broadcasting (DVB-T), and is also proposed for next-generation high-bandwidth systems such as Ultra Wideband (UWB). A similar baseband implementation, discrete multitone (DMT), is already widely used in copper-based Digital Subscriber Line (DSL) systems [5]–[9]. Considering the industry's extensive experience and the large economies of scale, OFDM and DMT are seen as promising technologies for low-cost, reliable, and robust Gigabit transmission over SI-POF.

This paper focuses on the application of DMT over IM/DD SI-POF links and shows the use of bit-loading in order to maximize the achievable transmission rate. The organization of the paper is as follows: starting with a short introduction to the principle of DMT modulation, a mathematical model for DMT transmission over SI-POF is then derived and used for calculating the Shannon capacity of a typical SI-POF system. Subsequently, a more realistic numerical approach is used to compute the achievable capacity when DMT is applied over SI-POF, based on measured frequency response values combined with the use of the optimum rate-adaptive water-filling algorithm

Manuscript received July 31, 2008; revised November 26, 2008. First published April 24, 2009; current version published May 13, 2009. This work was supported in part by the E.U. Government under Grant IST-FP6 STREP, nr. 027549, POF-ALL.

S. C. J. Lee, H. P. A. van den Boom, and A. M. J. Koonen are with the COBRA Research Institute, Eindhoven University of Technology, 5600 MB, Eindhoven, the Netherlands (e-mail: s.c.j.lee@tue.nl; h.p.a.v.d.boom@tue.nl; a.m.j.koonen@tue.nl).

F. Breyer is with the Institute of Communications Engineering, Technische Universität München, 80333 Munich, Germany (e-mail: florian.breyer@tum.de).

S. Randel is with Corporate Technology, Information and Communications, Siemens AG, Munich 80333, Germany (e-mail: sebastian.randel@siemens.com).

R. Gaudino and G. Bosco are with the Dipartimento di Elettronica, Politecnico di Torino, Torino 10129, Italy (e-mail: roberto.gaudino@polito.it; gabriella.bosco@polito.it).

A. Bluschke, M. Matthews, P. Rietzsch, and R. Steglich are with Teleconnect GmbH, Dresden 01157, Germany (e-mail: blua@teleconnect.de; blua@teleconnect.de; blua@teleconnect.de; blua@teleconnect.de).

Color versions of one or more of the figures in this paper are available online at http://ieeexplore.ieee.org.

Digital Object Identifier 10.1109/JLT.2009.2013480

[14]. Furthermore, it is shown how a derivative of this algorithm can be used to compute bit-loading, an important feature used to achieve near-optimum performance in DMT transmission systems. Experiments using DMT and bit-loading are then performed over different lengths of SI-POF and the results are compared to the theoretical and numerical capacity values. Finally, a real-time DMT over SI-POF system based on VDSL2 chipsets is presented and its performance is evaluated.

II. Principle of DMT Modulation

DMT is a multicarrier modulation technique where a high-speed serial data stream is divided into multiple parallel lower-speed streams and modulated onto subcarriers of different frequencies for transmission [10]. Usually, each subcarrier stream is mapped onto complex values C_n according to an M-ary quadrature amplitude modulation (M-QAM) constellation mapping, where $n = 1,2,\ldots,N-1$ denotes the subcarrier number and $N-1$ is the total number of data-carrying subcarriers used for transmission.

By using the inverse discrete Fourier transform (DFT) to modulate C_n onto different subcarrier frequencies, the resulting subcarriers are mutually orthogonal. In practice, the fast Fourier transform (FFT) algorithm is used to efficiently implement the DFT function. Furthermore, when the $N-1$ information symbols C_n $(n = 1,2,\ldots,N-1)$ are used as input values for a $2N$-point inverse FFT (IFFT), where $C_0 = C_N = 0$ and the Hermitian symmetry property:

$$C_{2N-n} = C_n^* \tag{1}$$

is satisfied, the resulting output multicarrier DMT time-domain sequence s_k can be written as

$$s_k = \frac{1}{\sqrt{2N}} \sum_{n=0}^{2N-1} C_n \exp\left(j2\pi k \frac{n}{2N}\right), \quad k = 0,1,\ldots,2N-1. \tag{2}$$

The resulting s_k is a real-valued, baseband multicarrier signal consisting of $2N$ sample points.

The resilience of DMT in a dispersive channel is the result of parallel transmission and cyclic prefix. Due to parallel transmission of the data, the symbol period is much longer than in the case of standard serial transmission. Therefore, intersymbol interference (ISI) affects only a small fraction of a symbol period. By use of a cyclic prefix, this ISI can be easily eliminated and orthogonality among the subcarriers is ensured [4].

At the receiver, demodulation of the DMT sequence is then accomplished by using a $2N$-point FFT, resulting in

$$\hat{C}_n = \sum_{k=0}^{2N-1} \hat{s}_k \exp\left(-j2\pi k \frac{n}{2N}\right), \quad n = 0,1,\ldots,2N-1. \tag{3}$$

With a one-tap equalizer, the magnitude and phase shift of each subcarrier (as a result of channel impulse response) can be corrected and the information symbols $\hat{C}_n$ recovered after demodulation with the FFT.

III. Analysis of SI-POF Channel Capacity

A. Channel Model for DMT Over SI-POF

Before analyzing the capacity of an SI-POF system, the transmitter, channel, and receiver model should first be considered. For a large number of subcarriers (>10), a DMT time signal $x(t)$ can be modelled as a zero-mean, Gaussian-distributed process with variance σ_x^2 [6]. In order to efficiently transmit the DMT signal over an IM/DD channel such as SI-POF, the signal has first to be limited in amplitude [7]–[9]. A common and straightforward method to realize this is by clipping the waveform, resulting in a clipped electrical DMT signal $x(t)$

$$x(t) = \begin{cases} x_0(t), & |x_0(t)| \le A \\ A \cdot \exp\left(j \cdot \arg\left\{x_0(t)\right\}\right), & |x_0(t)| > A, \end{cases} \tag{4}$$

where A is the maximum allowed amplitude level and $x_0(t)$ is the DMT signal before clipping. The amount of clipping is given by the clipping factor μ, which is defined as

$$\mu = \frac{A}{\sqrt{E\left\{x_0^2(t)\right\}}} \tag{5}$$

where $E\{x_0^2(t)\}$ denotes the average signal power of the DMT time signal $x_0(t)$ before clipping. Typical values for μ lie in the range of 2.5–3.5 [7]–[9]. In the rest of the analysis, the value of μ will be fixed to 3. It should hereby be mentioned that this is an approximation to a problem that would otherwise require mathematical tools that are beyond the scope of this paper [11].

After clipping, a constant dc bias is added to the electrical DMT signal $x(t)$ to ensure that it is unipolar and suitable for driving a light-emitting or laser diode. In this analysis, an ideal transmitter is assumed and the dc bias is set to the value A, as given in (4). This results in an instantaneous transmitted optical power $P_{\text{opt}}(t)$, which is represented by

$$\begin{aligned} P_{\text{opt}}(t) &= \alpha\left[A + x(t)\right] \\ &= \alpha\left[\mu \cdot \sqrt{E\left\{x_0^2(t)\right\}} + x(t)\right] \end{aligned} \tag{6}$$

where α is the electrical-to-optical conversion factor in [W/A]. For convenience, α is assumed to have a value of 1 and (6) therefore reduces to

$$P_{\text{opt}}(t) = \mu \cdot \sqrt{E\left\{x_0^2(t)\right\}} + x(t). \tag{7}$$

As $x(t)$ is a generic zero-mean signal, the average transmitted optical power P_{ave} is given by

$$P_{\text{ave}} = \mu \cdot \sqrt{E\left\{x_0^2(t)\right\}}. \tag{8}$$

After transmission over POF, the optical signal is detected by a photodetector which is assumed to consist of a photodiode and a transimpedance amplifier. The received electrical signal from the photodetector can be written as

$$V(t) = R \cdot G \cdot \alpha_F \cdot P_{\text{opt}}(t) \otimes h_F(t) \tag{9}$$

where R is the responsivity of the photodiode in [A/W], G is the transimpedance gain of the photodetector in [V/A], α_F is the fiber attenuation and $\otimes$ denotes the convolution between the transmitted optical power $P_{\text{opt}}(t)$ and $h_F(t)$. $h_F(t)$ represents the (normalized, electrical-to-electrical) fiber impulse response. Following measurement results given in [12], the SI-POF channel can be modeled as a Gaussian low-pass filter and its frequency response can thus be expressed as

$$|H_F(f)|^2 = e^{-\left(\frac{f}{f_0}\right)^2} \text{ with } f_0 = f_{3\text{dB}}/\sqrt{\ln 2} \tag{10}$$

where $f_{3\text{dB}}$ is the -3-dB bandwidth of the full electrical-to-electrical channel. At the receiver side, the only noise source in the system that is taken into account is additive white Gaussian noise, which represents the noise introduced by the transimpedance amplifier in the photodetector.

B. Theoretical Analysis of SI-POF Channel Capacity

Using the channel model derived in Section III-A, the Shannon capacity of the SI-POF channel is investigated. This is achieved by reviewing the theory for the evaluation of the channel capacity for the general case of a receiver characterized by additive white Gaussian noise with power spectral density $G_n(f)$, and a received useful signal with power spectral density $G_s(f)$. Following some advanced but well-known results from information theory [13], the resulting capacity in this case is given by maximizing the quantity

$$C \leq \int_{-\infty}^{+\infty} \frac{1}{2} \log_2 \left(1 + \frac{G_s(f)}{G_n(f)}\right) df \tag{11}$$

under the constraint

$$P_s = \int_{-\infty}^{+\infty} G_s(f) df. \tag{12}$$

The unknown in this problem is the "signal spectral distribution" $G_s(f)$ that solves this optimization problem.

The solution, based on Lagrange multipliers, is given in [13], and can be expressed by

$$G_s(f) = (\nu - G_n(f))^+ \tag{13}$$

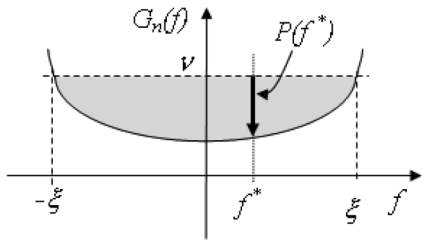

Fig. 1. Water-filling for POF channel.

where ν is an unknown value to be chosen so that

$$\int_{-\infty}^{+\infty} (\nu - G_n(f))^+ df = P_s \tag{14}$$

and $()^+$ is the functional giving the positive part of its argument, i.e.,

$$(z)^+ = \begin{cases} z, & \text{if } z \geq 0 \\ 0, & \text{if } z < 0 \end{cases} \tag{15}$$

This method is known in literature as water-filling [13], and has an intuitive explanation given in Fig. 1. For a given $G_n(f)$, finding ν in (13) means finding the "level" ν so that the area of the grey region in the figure is exactly equal to P_s. The meaning of the resulting optimal $G_s(f)$ is indicated in the figure using a thick arrow. Intuitively, the solution allocates most of the power in the frequency range where the noise is less. In particular, no power is allocated outside the "critical frequency" ξ, which satisfies the equation $G_n(\xi) = \nu$. This parameter ξ will play a key role in the following.

By combining (11) with the general result given by (13) and (14), the capacity of the SI-POF channel can be calculated. Neglecting the constant term P_{ave}, which does not carry any useful information, the received useful signal after photodetection has a power spectral density given by

$$G_I(f) = R^2 G^2 \alpha_F^2 \cdot |H_F(f)|^2 \cdot G_x(f) \tag{16}$$

where $G_x(f)$ is the power spectral density of the DMT signal $x(t)$, which is the "unknown" in the optimization problem and must satisfy the equality set by (12), which can be rewritten in the frequency domain as

$$\int_{-\infty}^{+\infty} G_x(f) df = E\left\{x^2(t)\right\}. \tag{17}$$

For a clipping factor $\mu \geq 3$, the mean power of a DMT signal before and after clipping is approximately the same. Therefore, $E\{x^2(t)\}$ is assumed to be equal to $E\{x_0^2(t)\}$ and (8) can be written as

$$E\left\{x^2(t)\right\} \cong E\left\{x_0^2(t)\right\} = (P_{\text{ave}}/\mu)^2. \tag{18}$$

Inserting (18) into (17) results in

$$\int_{-\infty}^{+\infty} G_x(f)df = (P_{\text{ave}}/\mu)^2 \tag{19}$$

which leads to the constraint that has to be met.

By considering flat receiver noise with power spectral density $N_0/2$ and using (11), the capacity of the POF channel can be written as

$$C \le \int_{-\infty}^{+\infty} \frac{1}{2}\log_2\left(1+\frac{R^2G^2\alpha_F^2\cdot G_x(f)\cdot|H_F(f)|^2}{N_0/2}\right)df \tag{20}$$

with bound given by (19). Equation (20) can be further simplified to

$$C \le \int_{-\infty}^{+\infty} \frac{1}{2}\log_2\left(1+\frac{2\alpha_F^2\cdot G_x(f)\cdot|H_F(f)|^2}{NEP^2}\right)df \tag{21}$$

with NEP defined as the noise equivalent power in [W/$\sqrt{}$Hz]. NEP is a commonly used figure of merit to characterize the noise performance of photodetectors. The optimization problem given by (19) and (21) is equivalent to the general case in (11) and (12) if we set

$$\begin{aligned} G_s(f) &= G_x(f),\\ G_n(f) &= \frac{NEP^2}{2\alpha_F^2}\cdot e^{\left(\frac{f}{f_0}\right)^2}. \end{aligned} \tag{22}$$

Using the "water-filling" technique given by (13) and (14), and by explicitly inserting the parameter ξ, the problem is rewritten as

$$\int_{-\xi}^{+\xi} (\nu - G_n(f))^+ df = P_s \tag{23}$$

with $\nu = G_n(\xi) = (NEP^2/2\alpha_F^2)\cdot e^{(\xi/f_0)^2}$, which can finally be formulated as

$$\frac{NEP^2}{2\alpha_F^2}\cdot\int_{-\xi}^{+\xi}\left(e^{\left(\frac{\xi}{f_0}\right)^2}-e^{\left(\frac{f}{f_0}\right)^2}\right)df = (P_{\text{ave}}/\mu)^2. \tag{24}$$

This turns out to be a nonlinear problem in the unknown ξ which can be solved numerically. After some algebraic passages shown in the Appendix, the following results arise.

— By introducing a new normalized parameter $\eta = \xi/f_0$, this parameter depends only on

$$\text{SNR}_{\text{eq}} = \frac{2\alpha_F^2\cdot P_{\text{ave}}^2}{NEP^2\cdot\mu^2\cdot f_0} \tag{25}$$

through a nonlinear law $\eta = g(\text{SNR}_{\text{eq}})$ that can be easily computed numerically. SNR_{eq} represents an "equivalent" signal-to-noise ratio after photodetection.

— The resulting capacity has a closed form expression in η, given by

$$C = \frac{2}{3\ln(2)\sqrt{\ln(2)}} f_{3\text{dB}}\eta^3. \tag{26}$$

In conclusion, the capacity of the SI-POF channel can be calculated by

$$C = \frac{2}{3\ln(2)\sqrt{\ln(2)}} f_{3\text{dB}}\cdot g^3(\text{SNR}_{\text{eq}}) \tag{27}$$

which depends on the -3-dB bandwidth $f_{3\text{dB}}$ of the (Gaussian low-pass) channel and the equivalent signal-to-noise ratio SNR_{eq} given in (25). Fig. 2 gives a general curve for (27) by plotting $C/f_{3\text{dB}}$ as a function of SNR_{eq}. From this curve, it can be seen that for a system with $\text{SNR}_{\text{eq}} = 24$ dB, the resulting $C/f_{3\text{dB}}$ is approximately 10. This means that the channel capacity C in bit/s is 10 times larger than its -3-dB bandwidth $f_{3\text{dB}}$.

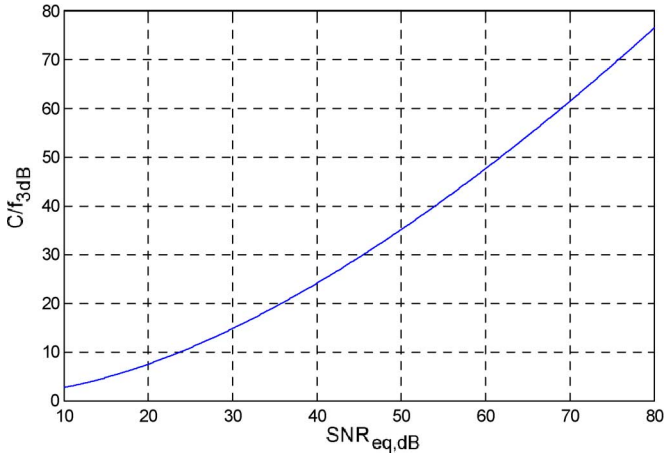

Fig. 2. Normalized capacity $C/f_{3\text{dB}}$ versus SNR_{eq}.

Using Fig. 2, the capacity of an SI-POF channel can be calculated if its $f_{3\text{dB}}$ is known. Therefore, measurements have been done to determine the $f_{3\text{dB}}$ of different lengths of SI-POF. For the measurements, a 655-nm DVD laser diode (LD) (500-MHz bandwidth) is used as transmitter and a Si-photodetector with transimpedance amplifier (300-MHz bandwidth) is used as receiver. Bandwidth limitation from both transmitter and receiver can therefore be neglected. The SI-POF used is a commercially available Mitsubishi ESKA GH4001, with a core-diameter of 1 mm, an NA of 0.5, and an attenuation of approximately 140 dB/km at 650 nm. The measured $f_{3\text{dB}}$ values for different lengths of SI-POF are listed in Table I, together with the channel capacity, calculated based on the following transmission characteristics.

— Average transmitted optical power: $P_{\text{ave}} = 2.5$ dBm.

— Fiber attenuation at 650 nm: $\alpha_F = 140$ dB/km.

— Clipping factor: $\mu = 3$.

TABLE I
CALCULATED THEORETICAL CAPACITY OF SI-POF AT 650 nm

Length (m)	Measured electrical -3dB bandwidth (MHz)	SNR_{eq} (dB)	Capacity (Gbit/s)
25	200	64	10.7
50	110	59	5.1
75	83	53	3.4
100	62	48	2.2
150	33	36	0.8
200	17	25	0.2

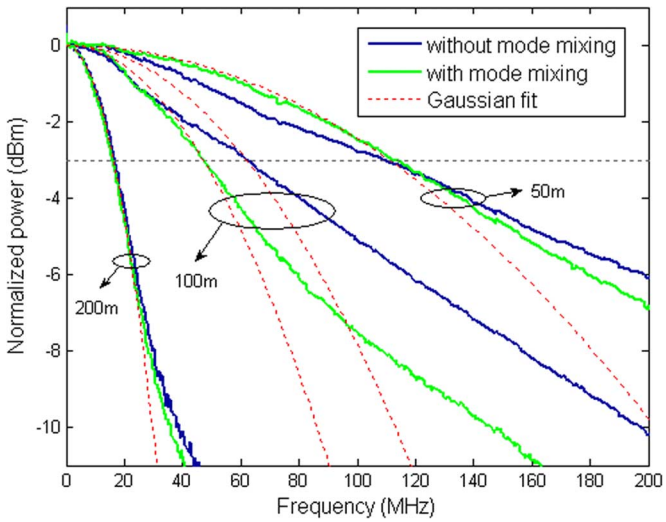

Fig. 3. Measured frequency response for different lengths of SI-POF with a 650-nm laser diode.

— Noise equivalent power: NEP $= 16 \cdot 10^{-12}$ W/$\sqrt{\text{Hz}}$.

From Table I, it can be seen that a capacity of 10 Gbit/s can be achieved for 25 m of SI-POF.

For comparison, the measured frequency response for 50, 100, and 200 m of SI-POF are depicted in Fig. 3. Although the frequency response of an SI-POF channel can be approximated well with a Gaussian low-pass function for lengths $\geq$200 m [12], it can be seen that the same does not apply for SI-POF with lengths $<$200 m. Especially when the LD is directly coupled to the SI-POF, a Gaussian approximation of the frequency response (dotted lines) results in large discrepancies at frequencies beyond the $-$3-dB point. This can clearly be seen from the curves measured with 100 and 50 m of SI-POF (blue lines). The difference is caused by mode coupling, where equilibrium mode distribution is not reached for SI-POF lengths $<$200 m. This is due to the low-NA launch by directly coupling the LD to the SI-POF.

However, when mode mixing is introduced at the beginning of the link by winding the SI-POF four times around a cylinder with a radius of 0.5 cm, the results (green lines) resemble the Gaussian approximation more. Nevertheless, it can be seen that a Gaussian low-pass is a pessimistic approximation of the SI-POF channel response for lengths $<$200 m. For 100 m of SI-POF, mode mixing reduces the channel bandwidth as a result of a larger amount of modal dispersion. In the case of 200 m of SI-POF, mode mixing does not influence the results very much, indicating that equilibrium mode distribution is reached after 200 m. From the results given in Fig. 3, it can be concluded that for lengths $<$200 m, a Gaussian approximation of the channel response leads to lower capacity values compared to the actual case. This is also the case when mode mixing is introduced at the beginning of the SI-POF. Therefore, actual capacity values of SI-POF can be larger than those calculated in Table I. However, these values still provide a good estimation for the SI-POF capacity.

C. DMT Over SI-POF Channel Capacity

Application of DMT over SI-POF requires the use of digital-to-analogue (DAC) and analogue-to-digital converters (ADC). Due to sampling speed limitations of both ADC and DAC, the capacity values shown in Table I may not be realistic when compared to an actual DMT over SI-POF system. In order to make a more realistic estimation of achievable SI-POF capacity values when DMT modulation is employed, a bandwidth-limited numerical approach should be used to reevaluate the achievable capacity.

The key aspect of DMT is to decompose a single frequency-selective communication channel into an equivalent multitone channel consisting of multiple parallel frequency-flat subchannels. By limiting the SI-POF system's bandwidth to f_B as a result of DAC and ADC sampling speed and dividing the frequency response into N subchannels, the optimization problem given in (11) and (12) can be reformulated [14] as a problem of maximizing the total achievable bit-rate b

$$\max_{\mathrm{E}_n} b = \sum_{n=1}^{N'} \frac{1}{2} \log_2 \left(1 + \frac{\mathrm{SNR}_n}{\Gamma}\right) \tag{28}$$

which is the sum of the bit-rates of all N' subchannels used for transmission. In (28), $\mathrm{SNR}_n = E_n \cdot g_n$ is the signal-to-noise ratio (SNR) of each subchannel, where g_n represents the subchannel SNR when unit energy is applied, Γ is the difference (gap) between the SNR needed to achieve maximum capacity and the SNR to achieve this capacity at a given bit error probability, and E_n is the allocated energy per subchannel, subject to an energy constraint given by

$$\sum_{n=1}^{N'} E_n = E_{\mathrm{tot}}. \tag{29}$$

E_{tot} is the fixed total available energy for transmission. The problem is now to find the optimum number of bits per subchannel, and the corresponding energy distribution per subchannel E_n, in order to maximize the bit-rate. From (28) and (29), it can be seen that N', the total number of subchannels used to achieve maximum bit-rate, does not need to correspond to the total number of available subchannels N. Therefore, the optimal solution is not always to use all available subchannels to transmit information.

Similar to (14), the solution is the water-filling method. In this case, the solution is computed numerically using the optimum rate-adaptive water-filling algorithm as described in [14].

TABLE II
COMPARISON OF DMT OVER SI-POF CAPACITY AT 650 nm

Length (m)	Theoretical Capacity from Table I (Gbit/s)	Numerical DMT over SI-POF Capacity (Gbit/s)	Measured Capacity (Gbit/s) @ BER = $1{\cdot}10^{-3}$
25	10.7	5.3	2.0
50	5.1	4.4	1.6
75	3.4	3.6	1.5
100	2.2	2.6	1.4
150	0.8	0.8	0.4
200	0.2	0.2	0.1

This algorithm computes the maximum achievable bit-rate b for a given communication channel when the SNR per subchannel is known. Due to this numerical approach, the measured frequency response values of different lengths of SI-POF are used for the computation, instead of an analytical Gaussian low-pass approximation. The considered system bandwidth f_B is limited to a Nyquist frequency of 312.5 MHz, which corresponds to the maximum sampling speed of the DAC (625 MSamples/s) used for measurements that will be described in Section IV. Moreover, in order to have realistic values for g_n, the noise power spectral density of the photodetector used for the measurements is measured and considered in the computation as well.

Table II shows the results. Compared to the results given in Table I, it can be seen that for short lengths of SI-POF ($<$75 m), the numerically computed capacity values are lower than the theoretical values. This results from bandwidth limitation due to the DAC and ADC sampling speeds, considered in the computation. For lengths of 75 and 100 m, the capacity is larger because of the larger bandwidth available, compared to the Gaussian approximation used in the calculation. For lengths $>$100 m, the measured frequency responses resemble the Gaussian approximation more and the SI-POF bandwidth dominates above the DAC and ADC sampling bandwidth. Therefore, the capacity values are similar to each other.

IV. VALIDATION WITH EXPERIMENTAL RESULTS

In order to validate the capacity values determined in Section III, experiments with DMT transmission over different lengths of SI-POF are performed.

A. Bit-Loading in DMT Modulation

An important feature of DMT is the possibility to allocate the number of bits per subchannel according to its SNR, typically known as bit-loading. There are two categories of bit-loading, rate-adaptive and margin-adaptive. Rate-adaptive algorithms maximize the bit rate for a fixed bit-error ratio (BER) and given power constraint, while margin-adaptive algorithms minimize the BER for a given bit rate. As the objective is to determine the achievable capacity over SI-POF, rate-adaptive bit-loading will be applied in order to maximize the transmission rate.

In Section III-C, the optimum rate-adaptive water-filling algorithm [14] was used to compute the maximum achievable bit-rate for the SI-POF channel by considering it as a multitone channel and allocating the optimum number of bits and energy to each subchannel. Similarly, this algorithm can also be used to compute optimum bit-loading in DMT modulation. However, infinite granularity for the number of bits per subchannel is assumed, resulting in non-integer values for the optimum number of bits per subchannel. Therefore, this algorithm is not suitable for practical implementation.

An alternative is to use suboptimal finite bit-loading algorithms, such as the Chow's rate-adaptive algorithm [15]. This algorithm is based on (28) and starts by discarding the subchannels that are least energy-efficient from information transmission, and redistributing the energy to more efficient subchannels to support higher data rates. The non-integer number of allocated bits per subchannel are then rounded to the nearest integer and the corresponding energy is in- or decreased to support the newly allocated number of bits at the same performance. Chow's algorithm has been shown to achieve near-optimum performance [14],[15] and will be used in the following to compute rate-adaptive bit-loading for DMT over SI-POF measurements.

B. DMT Transmission Over 100 m of SI-POF

Fig. 4 shows the experimental setup of DMT transmission over SI-POF. Using offline processing, a DMT time signal is computed and loaded into the memory of an Agilent N8241A arbitrary waveform generator (AWG). The AWG generates the analogue DMT waveform at a sampling speed of 625 MSamples/s and a resolution of 15 bits. The characteristics of the generated DMT waveform are:

— 256 subchannels, first channel at dc not used;
— 1.2 % cyclic prefix and 1 % preambles;
— 312.5-MHz bandwidth.

The analog electrical waveform from the AWG is then used to drive a low-cost, commercially available DVD laser diode (655 nm) with integrated ball lens. A dc-bias is added to the bipolar signal via a bias-tee in order to a have a unipolar signal, suitable for driving the laser diode. The mean transmitted optical power after coupling into 0.5 m of SI-POF is measured to be 2.5 dBm and the optical modulation amplitude (OMA), as defined in [16], is 5.4 dBm. The same SI-POF used previously for the frequency response measurements is now used for the DMT transmission experiment. After transmission over 100 m of SI-POF, the optical signal is detected by use of a photodetector with an integrated trans-impedance amplifier. The signal is then captured with a LeCroy Wavemaster 8500 A real-time digital storage oscilloscope with a nominal resolution of 8 bits and a sampling speed of 2.5 GSamples/s. This sampling speed is necessary due to the lack of a phase-locked loop and an appropriate low-pass filter. Additionally, oversampling enhances the effective resolution of the oscilloscope. The sampling clocks of the AWG and oscilloscope are free-running and not synchronized with a cable. In a practical system where properly designed components are available, sampling speeds closer to 625 MSamples/s can be used. The sampled DMT time sequence is then stored and demodulated using offline processing.

Initially, all subchannels are loaded with four information bits each, corresponding to a modulation format of 16-QAM. From the received and demodulated DMT signal, the SNR per subchannel is estimated [see Fig. 5(a)] and used to compute Chow's rate-adaptive bit-loading. This results in the bit-loading

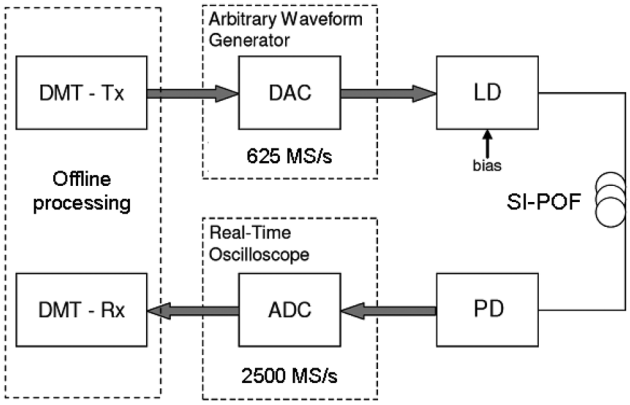

Fig. 4. Experimental setup for DMT over SI-POF. Tx: Transmitter; Rx: Receiver; LD: Laser diode; PD: Photodetector.

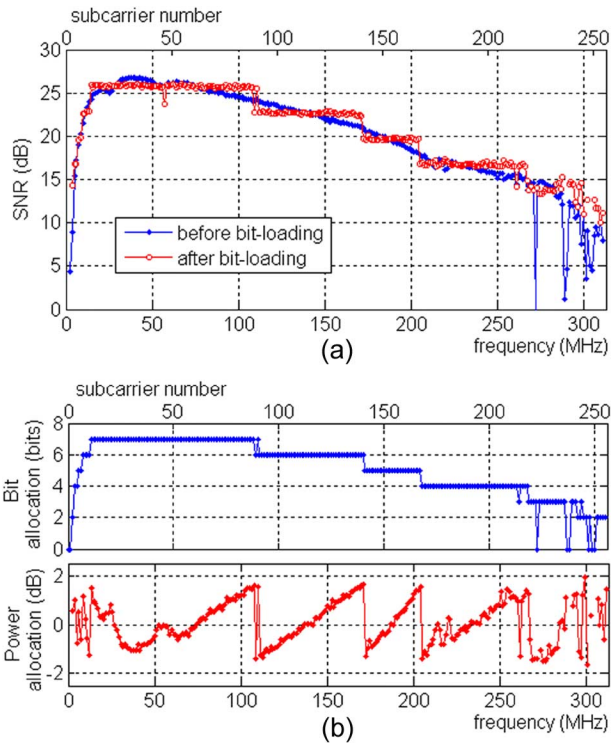

Fig. 5. DMT transmission characteristics for 100 m SI-POF. (a) Measured SNR per subchannel, before and after bit-loading. (b) Bit and power allocation per subchannel, resulting from bit-loading.

scheme per subchannel as depicted in Fig. 5(b). Note the saw-tooth-like power allocation scheme, which is typical for Chow's bit-loading algorithm. It can be seen that the peak-to-peak power deviation is approximately 3 dB, corresponding to the increase of the required SNR for transmitting 1 additional information bit using QAM. As a result of power allocation, the stair-case-shaped SNR per subchannel after bit-loading can be noticed from Fig. 5(a).

An aggregate transmission bit-rate of 1.62 Gbit/s is hereby achieved for a total averaged BER of $1 \cdot 10^{-3}$. After deduction of cyclic prefix, preambles, and 7 % error-correction coding, a net transmission bit-rate of 1.44 Gbit/s is achieved using DMT modulation over 100 m of SI-POF.

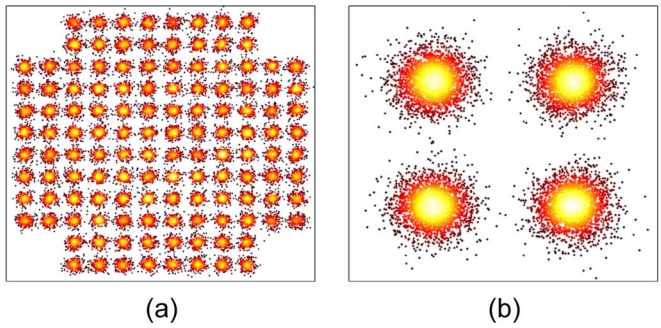

Fig. 6. Received constellations after transmission over 100 m of SI-POF. (a) 128-QAM, subchannel 29. (b) 4-QAM, subchannel 252.

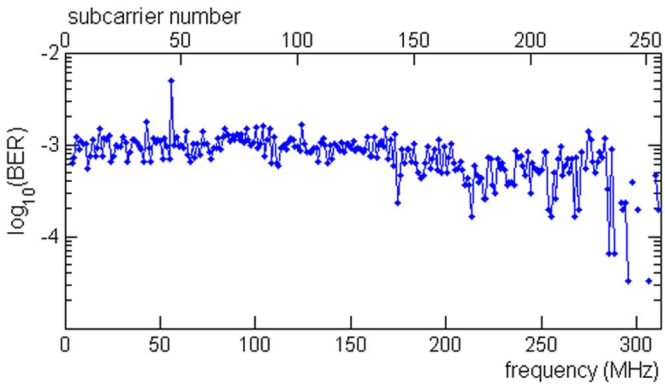

Fig. 7. Evaluated BER per subchannel. Total averaged BER $= 1 \cdot 10^{-3}$.

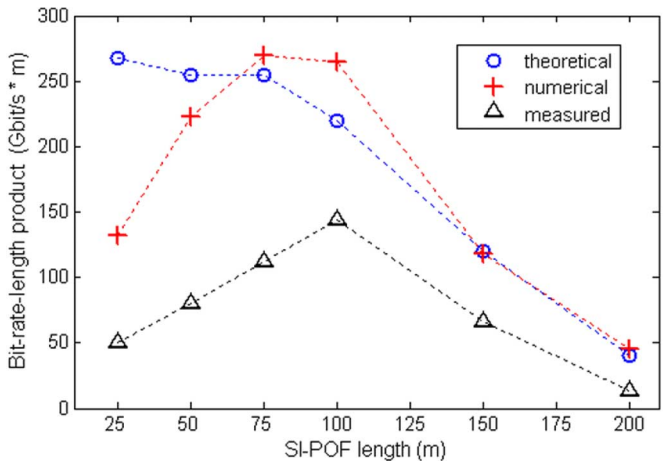

Fig. 8. Bit-rate-length product for theoretical, numerical, and measured capacity values of different lengths of SI-POF.

Fig. 6 shows two examples of received constellations for the highest and lowest allocated number of bits used for DMT transmission over 100 m of SI-POF. The BER performance per subchannel is plotted in Fig. 7, evaluated after transmission and reception of over 30 000 DMT frames (more than $30{\cdot}10^6$ bits). Because the serial data is transmitted in parallel over subchannels with DMT, the total uncoded BER of the received transmission data should be averaged from all subchannels and is calculated to be $1 \cdot 10^{-3}$.

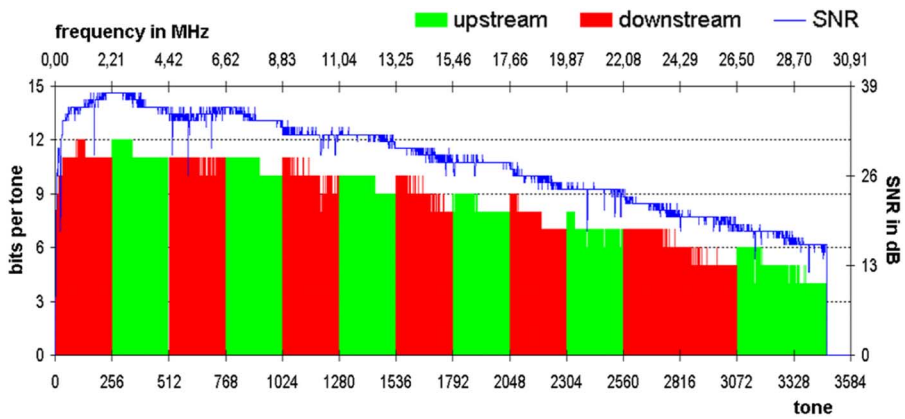

Fig. 9. Allocated number of bits per subchannel for up- and downstream DMT transmission over SI-POF.

C. DMT Over Different Lengths of SI-POF

Similar measurements with DMT transmission have been performed over different lengths of SI-POF using the same experimental setup shown in Fig. 4. The optical transmitted power and OMA are fixed at 2.5 and 5.4 dBm, respectively. The maximum achievable transmission rates at a BER of $1 \cdot 10^{-3}$ are listed and compared to the theoretical and numerical values in Table II.

Due to effects such as clipping, laser diode nonlinearity, quantization, and non-ideal sampling, additional noise is present in the measurement setup. Therefore, the achieved capacity values with measurements are lower than the theoretical and numerical values. Nevertheless, transmission rates of more than tenfold the -3-dB bandwidths are achieved using DMT and bit-loading over SI-POF.

By calculating the bit-rate-length products from the theoretical, numerical and measured capacity values, a better insight to the system performance can be gained. Fig. 8 shows these values as a function of the SI-POF length. For 75 and 100 m, the numerical values are higher than the theoretical values because the measured frequency response values were used for the simulations. These values have higher bandwidths than the Gaussian low-pass filter approximation for the frequency response used in the theoretical calculations, resulting in higher capacity values and bit-rate-length products. For lengths $<$75 m, the DAC and ADC sampling bandwidths limit the bit-rate-length products to values below the theoretical calculations (where only the SI-POF channel bandwidth is assumed). For lengths $>$100 m, the bandwidth-limitation is dominated by the SI-POF channel. Therefore, the values correspond more with each other.

Finally, it can be seen from the measured values that the highest bit-rate-length product is achieved for an SI-POF length of 100 m.

V. Real-Time Implementation of DMT Over SI-POF

In the previous sections, it has been shown that potentially high bit rates can be achieved over SI-POF using DMT. The next step is the implementation of a real-time DMT system and investigation of its performance over SI-POF. By use of commercially available xDSL chipsets based on DMT modulation, a real-time DMT over SI-POF transmission system can already be realized and first performance results can be evaluated. Consequently, an experimental demonstrator was built using state-of-the-art VDSL2 chipsets.

Using bit-loading based on (28) and the typical frequency response of 200 m of SI-POF, an optimized DMT band plan was computed, which is significantly different from the typical VDSL2 band plan for twisted-pair applications. In cooperation with VDSL2 chipset manufacturers, possibilities were found to modify the band plans by firmware changes. As a result, it was possible to optimize 12 bands up to a frequency of 30 MHz (3478 subchannels), as illustrated in Fig. 9. Unfortunately, due to the on-board Media Independent Interface (MII), the maximum bit-rate is limited to approximately 100 Mbit/s per direction. Therefore, the available bandwidth is split into an upstream and a downstream part. Furthermore, the subchannel spacing is fixed at 8625 kHz so that such a large number of subchannels have to be used in order to occupy the available bandwidth.

For the transmission experiment, optoelectronic interfaces based on green (520 nm) LEDs and large-area photodiodes were built. The experimental setup is depicted in Fig. 10. Due to the lack of optical SI-POF couplers, a bidirectional link comprising of two pieces of SI-POF (200 m each) was set up to test the computed band plan given in Fig. 9. The average transmitted optical power is 2.5 dBm and the SI-POF attenuation is approximately 83 dB/km at a wavelength of 520 nm. Using this configuration, a data rate of 101.832 Mbit/s upstream and 100.384 Mbit/s downstream is achieved. It should be noted that the system is fully compatible with Fast-Ethernet and has been tested according to this standard. First RFC2544 test results show an average latency of around 1.1 ms and 0 % packet loss for all packet sizes [17].

If the MII would allow, the sum of the up- and downstream data rates can be transmitted in one single direction, resulting in a total data rate of 202 Mbit/s for a single SI-POF of 200 m. When compared to the maximum capacity values shown in Table II, it seems that the maximum capacity is achieved. However, note that the values in Table II are for a wavelength of 650 nm, for which the SI-POF has a larger attenuation coefficient. When the calculation is made for a wavelength of 520 nm, a maximum theoretical capacity value of 540 Mbit/s is obtained.

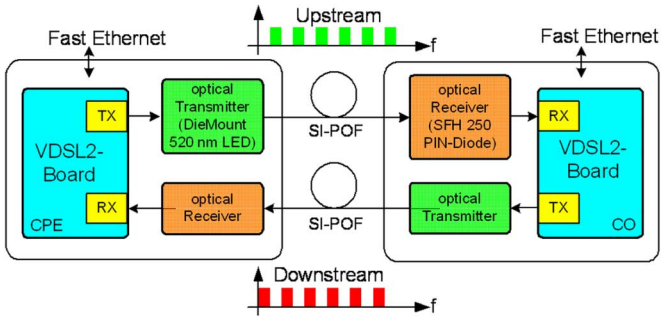

Fig. 10. Experimental setup of the DMT over SI-POF demonstrator based on VDSL2 chipsets. CPE: Customer Premises Equipment; CO: Central Office.

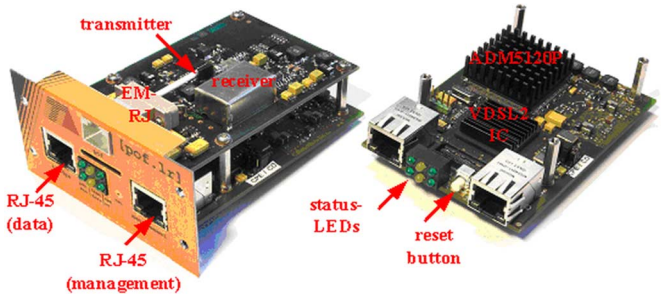

Fig. 11. Full working version of the DMT over SI-POF demonstrator, based on commercial VDSL2 chipsets, realized by Teleconnect.

Finally, Fig. 11 shows a picture of the full working DMT over SI-POF demonstrator, based on VDSL2 chipsets. This demonstrator is a media convertor that converts fast Ethernet from traditional unshielded twisted pair copper cables to SI-POF and achieves bidirectional transmission at a total bit-rate of 200 Mbit/s over a distance of 200 m. Compared to current commercial SI-POF systems, this media converter offers a twofold performance enhancement in both transmission rate and distance.

VI. Conclusion

In this paper, the water-filling method has been used to evaluate and calculate the Shannon capacity of the SI-POF channel. Additionally, a numerical frequency-discrete water-filling algorithm [14] is used to calculate more realistic capacity values subject to the constraint of DAC and ADC sampling bandwidths. Using rate-adaptive bit-loading to compute near-optimum bit-allocation schemes, the maximum achievable transmission rate of DMT over SI-POF is measured and evaluated. The results correspond well to the theoretical and numerical values. Moreover, a first real-time DMT over SI-POF system operating bidirectionally at 200 Mbit/s has been presented and its performance discussed. These results show that DMT is a promising solution for high-speed transmission over SI-POF.

Appendix

This appendix shows the main mathematical passages that lead to the capacity result shown in (27). First, an analytical expression for the capacity in terms of the parameter ξ is found. Starting from (14) and combining it with (23), the following is obtained:

$$\begin{aligned} C &= \int_{-\xi}^{\xi} \frac{1}{2}\log_2\left(1+\frac{\nu - G_n(f)}{G_n(f)}\right) df \\ &= \int_{-\xi}^{\xi} \frac{1}{2}\log_2\left(\frac{\nu}{G_n(f)}\right) df \\ &= \int_{-\xi}^{\xi} \frac{1}{2}\log_2\left(\frac{e^{\left(\frac{\xi}{f_0}\right)^2}}{e^{\left(\frac{f}{f_0}\right)^2}}\right) df \\ &= \frac{1}{2\cdot\ln 2}\int_{-\xi}^{\xi}\left(\frac{\xi^2 - f^2}{\ln 2 f_0^2}\right) df \\ &= \frac{2}{3\cdot\ln(2)}\frac{\xi^3}{f_0^2} \end{aligned} \tag{30}$$

By introducing $\eta = \xi/f_0$, the expression for the capacity can be written as

$$C = \frac{2}{3\cdot\ln(2)} f_0\cdot\eta^3 = \frac{2}{3\cdot\ln(2)\sqrt{\ln(2)}} f_{3\text{dB}}\cdot\eta^3. \tag{31}$$

The only remaining point is the evaluation of the quantity η. Starting from (24) and rewriting it introducing the parameter η results in

$$\begin{aligned} &\frac{NEP^2}{2\alpha_F^2}\cdot\int_{-\xi}^{+\xi}\left(e^{\left(\frac{\xi}{f_0}\right)^2} - e^{\left(\frac{f}{f_0}\right)^2}\right) df = (P_{\text{ave}}/\mu)^2 \\ &\frac{NEP^2}{2\alpha_F^2}\left(2f_0\eta e^{\eta^2} - f_0\int_{-\eta}^{+\eta} e^{w^2} dw\right) = (P_{\text{ave}}/\mu)^2 \\ &\Rightarrow 2\eta e^{\eta^2} - \int_{-\eta}^{+\eta} e^{w^2} dw = \frac{2\alpha_F^2\cdot P_{\text{ave}}^2}{NEP^2\cdot\mu^2\cdot f_0} \\ &\Rightarrow 2\eta e^{\eta^2} - \int_{-\eta}^{+\eta} e^{w^2} dw = \text{SNR}_{\text{eq}}. \end{aligned} \tag{32}$$

This last equation is the key equation for calculating the Shannon capacity of the SI-POF channel in this paper. It is to be meant as an equation in the unknown η. The only input to this equation is SNR_{eq}, so that in the end η is simply a given function of SNR_{eq}, i.e., $\eta = g(\text{SNR}_{\text{eq}})$. This function $g(\cdot)$ does not have a closed-form expression, but involving very smooth and regular functions can be very easily evaluated numerically.

References

[1] "Lightwave online," Infineon Unveils POF to Ethernet Transceiver Reference Design for Home Networking, May 17, 2006 [Online]. Available: http://lw.pennnet.com/articles/article_display.cfm

[2] S. Randel, S. C. J. Lee, B. Spinnler, F. Breyer, H. Rohde, J. Walewski, A. M. J. Koonen, and A. Kirstädter, "1 Gbit/s transmission with 6.3 bit/s/Hz spectral efficiency in a 100 m standard 1 mm step-index plastic optical fiber link using adaptive multiple sub-carrier modulation," presented at the Eur. Conf. Opt. Commun., Cannes, France, 2006, Post-deadline Paper Th4.4.1.
[3] F. Breyer, S. C. J. Lee, S. Randel, and N. Hanik, "1.25 Gbit/s transmission over up to 100 m standard 1 mm step-index polymer optical fiber using FFE or DFE equalisation schemes," presented at the Eur. Conf. Opt. Commun., Berlin, Germany, 2007, paper 9.6.6.
[4] R. van Nee and R. Prasad, *OFDM for Wireless Multimedia Communications*. Norwood, MA: Artech House, 2000.
[5] *Asymmetric Digital Subscriber Line (ADSL) Transceivers*, ITU Standard G.992.1, Jul. 1999.
[6] D. J. G. Mestdagh, P. Spruyt, and B. Biran, "Analysis of clipping effects in DMT-based ADSL systems," in *Proc. IEEE Int. Conf. Commun.'94*, 1994, pp. 293–300.
[7] J. M. Tang and K. A. Shore, "Maximizing the transmission performance of adaptively modulated optical OFDM signals in multimode-fiber links by optimizing analog-to-digital converters," *J. Lightw. Technol.*, vol. 25, no. 3, pp. 787–79, Mar. 2007.
[8] S. C. J. Lee, F. Breyer, S. Randel, H. P. A. van den Boom, and A. M. J. Koonen, "High-speed transmission over multimode fiber using discrete multitone modulation [Invited]," *J. Opt. Netw.*, vol. 7, pp. 183–196, 2008.
[9] S. C. J. Lee, F. Breyer, S. Randel, O. Ziemann, H. P. A. van den Boom, and A. M. J. Koonen, "Low-cost and robust 1-Gbit/s plastic optical fiber link based on light-emitting diode technology," in *OFC*, San Diego, CA, 2008, p. OWB3.
[10] J. M. Cioffi, Jun. 1, 2008, A Multicarrier Primer. [Online]. Available: http://www-isl.stanford.edu/~cioffi/pdf/multicarrier.pdf
[11] R. You and J. Kahn, "Upper-bounding the capacity of optical IM/DD channels with multiple-subcarrier modulation and fixed bias using trigonometric moment space method," *IEEE Trans. Inf. Theory*, vol. 48, no. 2, pp. 514–523, Feb. 2002.
[12] D. Cárdenas, A. Nespola, P. Spalla, S. Abrate, and R. Gaudino, "A media converter prototype for 10-Mb/s ethernet transmission over 425 m of large-core step-index polymer optical fiber," *J. Lightw. Technol.*, vol. 24, no. 12, pp. 4046–4052, Dec. 2006.
[13] R. G. Gallager, *Information Theory and Reliable Communication*. New York: Wiley, 1968.
[14] J. M. Cioffi, Jun. 1, 2008, Advanced Digital Communication, Course Reader. [Online]. Available: http://www.standford.edu/class/ee379c
[15] P. S. Chow, J. M. Cioffi, and J. A. C. Bingham, "A practical discrete multitone transceiver loading algorithm for data transmission over spectrally shaped channels," *IEEE Trans. Commun.*, vol. 43, no. 2, pp. 773–775, Feb. 1995.
[16] "Application Note 2710, HFAN-02.2.2: Optical Modulation Amplitude and Extinction Ratio," Sep. 15, 2003. [Online]. Available: http://www.maxim-ic.com/appnotes.cfm/an_pk/2710
[17] The Internet Engineering Task Force (IETF), "Benchmarking Methodology for Network Interconnect Devices" [Online]. Available: http://www.ietf.org/rfc/rfc2544.txt

S. C. Jeffrey Lee (S'06) received the M.Sc. degree in electrical engineering from the University of Technology Eindhoven (TU/e), Eindhoven, the Netherlands, in 2005. He is currently working towards the Ph.D. degree at Siemens AG, Munich, Germany, in collaboration with the TU/e.

In 2003, he started his research with an internship at NTT Photonics Laboratories, Atsugi, Kanagawa, Japan, where he worked on the design and characterization of electro-optical phase modulators. Following that, he conducted his Master's thesis work at Siemens AG in Munich, Germany, dealing with electrical gain control of Erbium-doped fiber amplifiers for long-haul fiber-optic transmission systems. He has authored and coauthored more than 30 refereed papers and conference contributions, including five invited papers and a book chapter. His current research is focused on advanced modulation techniques such as OFDM and DMT for multimode glass fibers, polymer optical fibers, and optical wireless communications.

Florian Breyer (S'06) received the Dipl.-Ing. degree in electrical engineering from Stuttgart University of Technology, Stuttgart, Germany, in 2005.

Since then, he has been with the Institute for Communications Engineering, Technische Universität München (TUM), Munich, Germany, in cooperation with Siemens Corporate Technology, as a Research and Teaching Assistant. His research interests are modeling and equalization schemes for optical transmission systems with polymer optical fiber.

Sebastian Randel (S'02–M'06) received the Dipl.-Ing. and the Dr.-Ing. degree from the Technical University Berlin, Berlin, Germany, in 2001 and 2005, respectively. His dissertation work dealt with physical layer issues of future WDM transmission systems operating at 160 Gbit/s per wavelength channel.

In 2005, he joined Siemens AG, Corporate Technology, Munich, Germany, as a Research Scientist. Currently, he is involved in research activities on polymer optical fibers, optical wireless communications, cost-efficient access network architectures, as well as advanced modulation formats for transport networks.

Roberto Gaudino (M'98) was born in Torino, Italy, in 1968.

He is currently an Associate Professor in the Optical Communication Group, Politecnico di Torino, Turin, Italy, where he works on several research topics related to optical communications. His main research interest is in the metro and long-haul DWDM systems, fiber nonlinearity, modeling of optical communication systems, and on the experimental implementation of optical networks. Currently, he is investigating on new optical modulation formats, such as polarization or phase modulation, and on packet switched optical networks. He spent one year in 1997 at the Georgia Institute of Technology, Atlanta, as a Visiting Researcher in the OCPN Group, where he worked in the realization of the MOSAIC optical network testbed. In 1998, was with the team that coordinates the development of the commercial optical system simulation software OptSim for two years. He is author or coauthor of more than 80 papers in the field of optical fiber transmission and optical networks, he is continuously involved in consulting for several companies of the optical sector, and he is also involved in professional continuing education. He is currently the coordinator of two EU STREP projects specifically focused on POF, titled "POF-ALL," and "POF-PLUS."

Gabriella Bosco (S'00–M'02) was born in Ivrea, Italy, in 1973. She received the Degree in telecommunication engineering in 1998 with a thesis on the nonlinear effect of the propagation in WDM optical systems and the Ph.D. degree in electronic and communication engineering in 2002 with a thesis on the performance analysis of optical communication systems, both from Politecnico di Torino, Turin, Italy.

In 2000, she was a Visiting Researcher at Optical Communication and Photonic Network (OCPN) Group, University of California, Santa Barbara, directed by Prof. Blumenthal, working on polarization-mode dispersion monitoring techniques. She currently holds a postdoctoral position in the Optical Communication Group, Department of Electronics, Politecnico di Torino. Her main research interests are focused on the performance analysis of optical transmission systems and the application of MLSE techniques in optical links.

Andreas Bluschke (M'07) received the Dipl.-Ing. and Dr.-Ing. degrees from the Leningrad Electrical Institute of Communication (LEIC), Leningrad, USSR, in 1982 and 1986, respectively.

He is cofounder and is currently the Managing director of Teleconnect GmbH, Dresden, Germany, since 1990. He is particularly responsible for R&D activities and is an experienced project leader in the areas of PDH, SDH, ISDN, and ATM with his main focus being xDSL. From 1986 to 1988, he worked as an Assistant at Hochschule für Verkehrswesen Dresden and was a Development Engineer at ZFTN Dresden from 1988 to 1990. He is author and editor of numerous books and journal articles on the topic of xDSL and access networks.

Michael Matthews received the Dipl.-Ing. degree from the Technical University of Chemnitz, Chemnitz, Germany. Since 1998, he has been working for Teleconnect GmbH, Dresden, Germany, as a Hardware and Software Development Engineer. He has been engaged in the field of xDSL systems for many years and has published several professional articles on this topic. Together with Dr. Bluschke, he is author of the Teleconnect GmbH's "xDSL-Homepage" (http://xdsl.teleconnect.de) and editor of the book *xDSL-Fibel* (Vde-Verlag, 2001).

Philipp Rietzsch rfeceived the Dipl.-Ing. (FH) and M.Sc. degrees from the University of Applied Sciences, Dresden, Germany, in 2005 and 2007, respectively.

He has been working for Teleconnect GmbH since 2005 as a Hardware and Software Development Engineer, focusing on xDSL systems. Together with Dr. Bluschke and Michael Matthews, he has authored and coauthored various publications.

Rainer Steglich is currently pursuing the electrical engineering degree (specialization in communication technologies) since 2005 at the University of Applied Sciences (FH) Mittweida, Germany.

He is currently doing his internship at the chair of Communication Technology, in collaboration with Teleconnect GmbH.

Henricus P. A. van den Boom was born in Eindhoven, The Netherlands, in 1955. He received the degree of Elektrotechnisch Ingenieur from the Eindhoven University of Technology, Eindhoven, in 1984.

Since then, he has been an Assistant Professor at the Electro-Optical Communications Group, Department of Electrical Engineering, Eindhoven University of Technology. He lectures in basic telecommunication theory and optoelectronic communication systems and networks. He has been involved in research on coherent optical communication systems, optical cross-connected networks and broadband communications in hybrid fiber coax networks. Currently, he is working on polymer optical fiber systems and networks.

Antonius M. J. Koonen (M'00–SM'01–F'07) received the M.Sc. (*cum laude*) in electrical engineering from the Eindhoven University of Technology, Eindhoven, The Netherlands, in 1979.

He spent more than 20 years at Bell Laboratories in Lucent Technologies as a Technical Manager of Applied Research. He has also been a Bell Labs Fellow since 1998 (the first one in Europe). Next to his industrial position, he has been a part-time Professor at Twente University from 1991 to 2000. Since 2001, he has been a Full Professor at the Eindhoven University of Technology in the Electro-Optical Communication Systems group, which is a partner in the COBRA Institute; since 2004, he has been the Chairman of this group.

His main interests are currently in broadband fiber access networks and in optical packet-switched networks. He has initiated and led several European and national R&D projects in this area, on label-controlled optical packet routed networks (the EC FP5 IST project STOLAS), dynamically reconfigurable hybrid fiber access networks (EC FP4 ACTS TOBASCO on fiber-coax, EC FP4 ACTS PRISMA on fiber-wireless, EC FP5 IST HARMONICS on packet-switched access), and short-range multimode (polymer) optical fiber networks. Currently, he is involved in a number of access/in-home projects in the Dutch Freeband program, in the Dutch IOP Generieke Communicatie program, and in the EC FP6 IST Broadband for All program (MUSE, e-Photon/ONe+, POF-ALL).